

Micro-fiber elements as perfusive catalysts or in catalytic mixers

Flow, mixing and mass transfer

J. De Greef, G. Desmet, G.V. Baron*

Vrije Universiteit Brussel, Department of Chemical Engineering Pleinlaan 2, Brussels 1050, Belgium

Available online 11 July 2005

Abstract

The flow, mixing and mass transfer in a catalytic stirrer containing catalyst coated porous micro-fiber elements, based on a concept introduced by Moulijn, were studied in a lab-scale reactor with 13 samples of materials with fiber diameters from 8 to 35 μm and porosity values between 0.60 and 0.90. Pressure drop in these sintered metallic fiber materials was shown to follow a modified Kozeny–Carman equation:

$$\frac{\Delta P}{L} = \left[2 + 0.053 \left(\frac{\varepsilon}{1 - \varepsilon} \right)^3 \right] \mu \frac{16}{d_f^2} \frac{(1 - \varepsilon)^2}{\varepsilon^3} u_0$$

When rotating in the reactor, the flow through the fiber mats can be estimated from

$$u^{-1} = \frac{\tau}{L} = 32 \frac{\mu L}{\alpha_D \rho d_f^2} \left[2 \frac{(1 - \varepsilon)^2}{\varepsilon^3} + \frac{0.053}{(1 - \varepsilon)} \right] u_T^{-2}$$

where α_D is a drag coefficient of around 2.5. Flow through the catalyst in an operational stirrer can be adjusted over several orders of magnitude by manipulating parameters, such as rotational speed, dimension of the fiber stack and its material characteristics.

Mass transport between fibers and the liquid flow through fiber stacks follows:

$$\varepsilon Sh = 0.47 Re^{1/2} Sc^{1/3}$$

© 2005 Elsevier B.V. All rights reserved.

Keywords: Catalytic fibers, Catalytic stirrer

1. Introduction

Structuring catalysts offers many advantages over packed beds and this is probably even more so in liquid phase reactions [1]. Fibrous structures form a special category, and with their fine structure, interconnected space and high porosity, they would be especially suitable for liquid phase operation. Over the past decade, several

types of fibers have been catalytically activated by a variety of techniques [2,3].

The concept of a catalytic stirrer consisting of rotating monoliths for use in a CSTR was introduced, and successfully applied by Moulijn and co-workers [4]. Our aim was to investigate if fibrous mats could replace the monolith sections, and collect sufficient data to derive correlations and a design procedure for such systems. Integrated in the blades of the stirrer, the fiber elements do not only contribute to the mixing of a stirred tank reactor, but also simultaneously serve as a micro-structured

* Corresponding author. Tel.: +32 2 6293246; fax: +32 2 6293248.

E-mail address: gvbaron@vub.ac.be (G.V. Baron).

Nomenclature

A	fit parameter (see Eq. (4)) (m/s)
A_S	blade surface (m ²)
C^*	dimensionless (relative) concentration level (vessel + sample)
C_D	drag coefficient
d_f	fiber diameter (μm)
D_i	impeller diameter (m)
D	diffusion coefficient (m ² /s)
F_D	drag force (N)
h	convection mass transfer coefficient (m/s)
K_0	parameter (=2)
K	Kozeny constant
L	fiber sheet stacking length (m)
n	parameter
Re	Reynolds number, $Re = u_0 d_f / \nu$
Sc	Schmidt number, $Sc = \nu / D$
Sh	Sherwood number, $Sh = h d_f / D$
t	time (s)
t_d	delay time (s)
u	internal blade velocity (m/s)
u_T	tip speed (m/s)
u_0	superficial velocity in fiber stack (m/s)

Greek symbols

α_D	drag coefficient
ΔP	pressure drop (N/m ²)
ε	porosity
λ	reference length (=10 ⁻² m)
μ	dynamic viscosity (Pa.s)
ν	kinematic viscosity (m ² /s)
ρ	fluid density (kg/m ³)
τ'	characteristic flow-through time of a porous sample with reference length λ (s)
τ	characteristic flow-through time of porous sample (s)

permeable environment for catalyst immobilization. Fibrous media indeed offer an acceptable specific surface area to be coated with a mono-layer of micron sized catalyst particles, layers of noble metals, enzymes, etc. Therefore, the concept allows combining to a certain extent the favorable properties of a CSTR and PB elements in one single unit. A major advantage of the system is that it can easily be retrofitted on stirred tank reactors, currently used in the fine chemicals and the pharmaceutical industry, where the production usually occurs in small or large batches. The rotating porous parts of the experimental setup allow high values of porosities up to 90%, containing miniaturized open structures which eliminate the pressure-drop constraint, permit optimal reactor productivity for a flow frequently passing through the medium.

A type of sintered metallic fiber materials was characterized with regard to pressure drop. More specifically, flow related parameters of the system, such as residence time values and flow-through velocities in the blades are determined via dynamic tracer response experiments. Finally mass transfer from fiber to fluid was investigated.

2. Materials and set-up

A plexiglass lab-scale stirred tank reactor, with internal vessel diameter of 13 cm was used as experimental set-up (Fig. 1). The impeller consisted of two hollow plastic tubing sections (length = 1.5 cm and inner diameter = 2 cm) loaded with fibrous materials. The blades were fixed at 5 cm from the vessel bottom and the distance between the center of both blades amounted 7 cm. Circular slices ($d = 2$ cm) were cut from sintered metallic fiber sheets (Bekaert, Belgium) and closely stacked to form continuous porous elements with a length varying between 0.6 and 1.2 cm. This stack of fiber sheets was fixed in the tubing with stretchable parafilm-strips to ensure a nice fit into the stirring system and avoiding bypassing flow. The front and backside of the porous blade elements were left uncovered, allowing flow-through. Thirteen different fibrous materials were tested with fiber diameter ranging from 8 up to 35 μm and the porosity values were situated between 0.60 and 0.90. The stirrer system was driven by a motor with speed control (Applikon, Schiedam, The Netherlands), that allowed establishing rotational speeds between 20 and 600 rpm.

For each experimental run, one porous stirrer blade was pre-saturated with a 15 mM methylene blue tracer solution. The idea behind the measurement technique is that, for a sufficiently fast mixing of the tank fluid, the rate of colouring of the medium is equal to the rate of tracer release from the rotating blade and hence also equal to the flow-through velocity in the porous elements. For practical reasons, it was decided to measure the response of only one blade. Indeed,

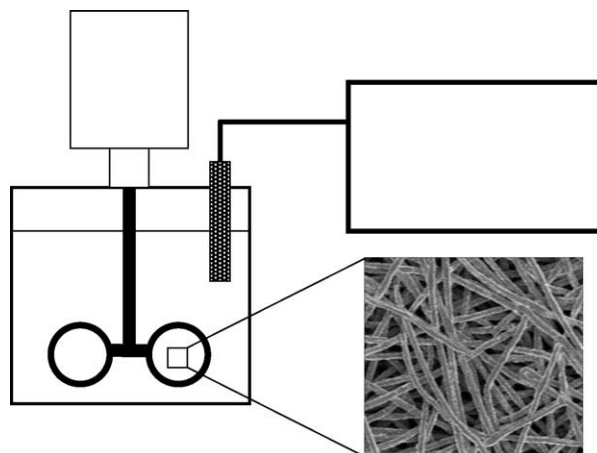


Fig. 1. Experimental set-up with stirred tank reactor.

due to limitations of the set-up, experimental differences in initiation time of tracer release between both blades prevented adequate response measurement of both blades at the same time.

After filling up the tank with a water volume of 2.4 l (fluid height = 18 cm), the preloaded stirrer system was gently put into its place in the tank, making sure that no tracer was released before starting the measurements. Via a probe connected to an online fiber optic spectrophotometer (MCPD-1000, Otsuka, Japan) the evolution of tracer concentration in the tank was recorded for various combinations of blade porosity, fiber diameter and stirrer tip speed.

3. Experimental method and signal modeling procedure

Since rotation of the stirrer induces a flow of tank fluid through the porous mixing blade, the characteristics of the tracer release from the saturated blade reveal the overall residence time inside the blade and hence the flow-through velocity. The response curve of tracer release was recorded for various fibrous materials.

As a representative example, in Fig. 2 a recorded signal is given for a 74% porous element with a fiber diameter of 8 μm , at a rotational speed of 200 rpm, i.e. a tip speed of 0.73 m/s. The measured signal is depicted as a thin line, while the thick line is a model curve, corresponding to a first order response. Especially at the lower rotational speeds, a small delay t_d appeared due to the imperfect vertical mixing in the tank, delaying the response at the detector, but the response remained in all cases first order, yielding a time constant τ .

$$C^*(t) = 1 - \exp\left(-\frac{t - t_d}{\tau}\right) \quad (1)$$

As mentioned earlier, the flow-through velocity in a rotating porous blade can be accurately measured if the mixing in the

surrounding tank fluid occurs much faster. The flow resistance and hence the flow velocity in the fibrous material then effectively determines the rate of colouring of the tank fluid. For the vast majority of the experimental runs, this condition was fulfilled and the tracer release signals as measured by the probe in the vessel were not significantly influenced.

To determine the conditions under which there is an influence of the tank mixing, exterior to the porous elements, the response for various tip speed values was recorded for a direct injection of tracer at the height of the porous stirrer blades. The tip speed is thereby defined as:

$$u_T = \frac{N\pi D_i}{60} \quad (2)$$

for which N is given in rpm and the impeller diameter $D_i = 7.10^{-2}$ m, i.e. the distance between the centers of both blades on the stirrer. The characteristic mixing time τ was determined for porous materials with varying fiber diameter and porosity. As could be expected because of the dimensions of the stirrer blades, the material characteristics hardly influenced the mixing time in the surrounding vessel medium. A correlation for τ (correlation coefficient = 0.985) was established (Fig. 3):

$$\tau = 0.89u_T^{-1} \quad (3)$$

For all experimental cases, the characteristic residence time τ of the tracer in the porous blade was accurately determined. An overview of the τ -values for all examined fibrous sample materials is given in Fig. 4. In order to withdraw the influence of a variable fiber sheet stacking length L in the stirrer blades, the characteristic time values are presented as a ratio τ/L , hereby assuming that the residence time scales in a linear way with respect to L (cf. discussion below). Evidently, the highest residence time values τ are achieved in fibrous media with the lowest porosity and the smallest fiber diameter (implying the narrowest flow-through pores), while the lowest residence time values go along with the highest porosities and the thickest fibers.

Some trends are remarkable. For a material with 63% porosity and $d_f = 8 \mu\text{m}$, the average time for an elementary

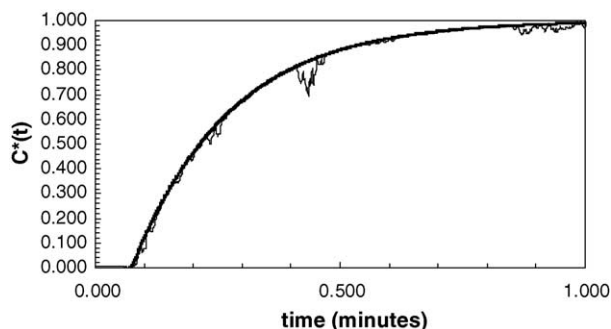


Fig. 2. Rescaled concentration release signal curve for a 74% porous mixing blade ($d_f = 8 \mu\text{m}$) at 200 rpm tip speed. The thin line represents the experimentally registered signal, while the thick curve corresponds with a first-order data fit (Eq. (1)).

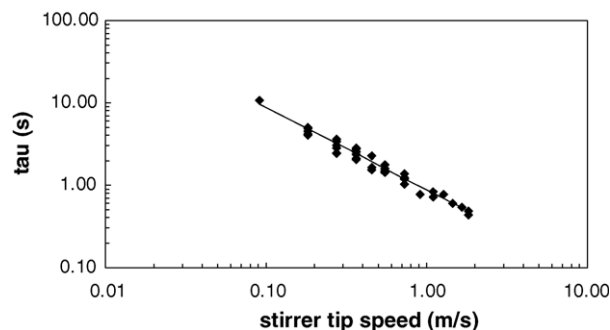


Fig. 3. Characteristic mixing times (τ) of the vessel medium, exhibiting inverted first-order dependency on the stirrer tip speed (data points collected from all experimental runs).

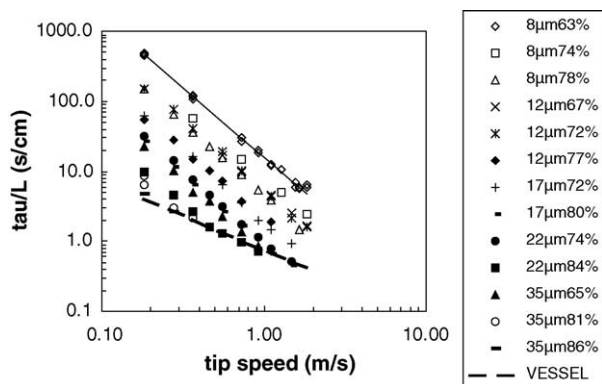


Fig. 4. Measured residence time values τ/L . The vessel mixing time (Eq. (3)) is indicated by the thick dashed bottom line. A second-order inverted relationship (Eq. (4)) on the tip speed is illustrated by the thin upper line.

fluid volume to travel through $L = 1$ cm of medium amounts up to about 450 s at a stirrer speed of 50 rpm ($u_T = 0.18$ m/s). However, by increasing the tip speed up to 500 rpm ($u_T = 1.83$ m/s) this time value is reduced by a factor 100, i.e. a scale-down along u_T^{-2} . This is concluded for all materials, regardless the porosity or the fiber diameter. For the τ -values at high tip speeds a lower bound limit to the u_T^{-2} -relationship however appears. For combinations of a high ε , a high d_f and a high u_T -value, the assumption of $\tau \ll \tau_{\text{vessel}}$ no longer holds. It can be clearly seen from the data series for $d_f = 22 \mu\text{m}$ and $\varepsilon = 0.84$, that the u_T^{-2} trend shifts towards a u_T^{-1} dependency, i.e. the mixing time correlation determined by Eq. (3) (indicated as a dashed black line in Fig. 4). In fact, the detection at the probe in the vessel is now determined by the mixing time of the tank medium. Under the conditions wherein τ approaches the τ for the tank and wherein thus both characteristic time values determine the performance of the system, Eq. (4) is no longer valid.

The different series of measured time-values, when external mixing is not limiting, as shown in Fig. 4, could be accurately described by the equation

$$\frac{\tau}{L} = A u_T^{-2} \quad (4)$$

wherein A is a parameter determined by fit of each data series. An overview of the value of A and its variability versus ε and d_f is presented in Table 1.

Table 1
Fitted values of A (m/s)

Porosity	0.63	0.74	0.78
$d_f = 8 \mu\text{m}$	1580	810	495
Porosity	0.67	0.72	0.77
$d_f = 12 \mu\text{m}$	518	398	220
Porosity	0.72	0.80	
$d_f = 17 \mu\text{m}$	210	90	
Porosity	0.74	0.84	
$d_f = 22 \mu\text{m}$	104	34	
Porosity	0.65	0.81	0.86
$d_f = 35 \mu\text{m}$	76	25	(20) vessel limit

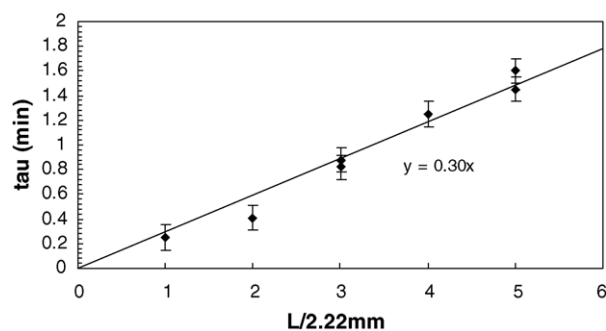


Fig. 5. Characteristic residence time in fiber sheet stacks with increasing length.

The fiber diameter, equally defining the dimensions of the flow-through pores, indeed also has a tremendous and straightforward effect on the fibrous blade permeability. Considering two materials with comparable porosity (0.63 and 0.65) but fiber diameters (respectively 8 and 35 μm) roughly differing with a factor 4.5, their characteristic time values at the lowest tip speed inversely scale with a factor 20, i.e. about the squared value of 4.5.

As mentioned above, the available amount of material differed for all fibrous samples, and the fiber stack length in the stirrer system could not be kept constant throughout all measurements. To check the validity of the assumption that τ scales linearly with L , a series of experimental runs was performed with a material with properties: $\varepsilon = 0.67$ and $d_f = 12 \mu\text{m}$. A steadily increasing number (from 1 to 5) of fiber sheet ‘packets’, having an individual length $L = 2.2 \times 10^{-3}$ m, were serially stacked up in a blade of the stirrer. For each (cumulative) length, the residence time τ_p was determined at a constant tip speed of 0.275 m/s (75 rpm), indeed revealing within the experimental error a constant ratio τ/L for an ever-increasing length of the fiber sheet stack (Fig. 5). The inverse of the slope, i.e. L/τ , is in fact an approximation of the overall fluid velocity in the porous sample. For the given case $u = L/\tau = 1.2 \times 10^{-4}$ m/s. This value is comparable with the inverse of the τ/L -value from Fig. 5, already measured earlier for a sample with identical specifications, i.e. 1.5×10^{-4} m/s.

4. Modeling of flow through catalytic stirrer

Although more rigorous modeling with CFD techniques is possible, a simple “first principles” model is presented, allowing estimation of the flow through the fiber mats when they are used in a catalytic stirrer of arbitrary shape. Let us consider a rotating blade as a stationary (porous) object in a flow (Fig. 6). This is in fact the complementary but equivalent representation of a blade rotating in the tank fluid. For further calculations, the fluid velocity approaching the stirrer blades is approximated by the tip speed u_T , although the real velocity in the direction of rotation may in fact be lower since the tank fluid will partly rotate with the stirrer.

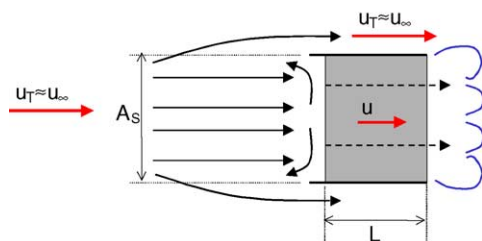


Fig. 6. Drag force induced flow-through.

Furthermore, since the time necessary for start-up is very short compared to the measured τ and since the maximal rotation velocity of the tank fluid is established very rapidly, we expect start-up effects to significantly influence only the measurement of the internal flow velocity through samples with a very low flow resistance, causing a fast tracer release (i.e. for the highest porosities and the thickest fiber diameters). As the flow rates through the fiber mats are then large, their exact knowledge for design is less critical.

The external flow exerts a force frontal to the blade and induces a flow (with velocity u) inside the porous object with length L . A counterforce originates from the internal fluid flow resistance and causes an unknown, but usually large fraction of the oncoming stream to deflect around the porous object. As the mass balance around the porous blade entrance hence is undetermined, the internal bed velocity must be derived from an averaged force (momentum) balance per unit of inlet area. In the porous blade, the flow gives rise to a pressure-drop between inlet and outlet.

Considering the stirrer blade to be a solid stationary object in a flow, the external kinetic resistance force exerted on the object can be written as the drag:

$$F_D = C_D A_s \frac{\rho u_T^2}{2} \quad (5)$$

As the blade is porous, the C_D will be different (α_D) but can still be assumed to follow the same type of relation. Moreover, only a fraction ε of this force acting on the inlet area induces a flow through the porous material, generating a pressure drop:

$$\Delta P = \alpha_D \varepsilon \frac{\rho u_T^2}{2} \quad (6)$$

The equation of Kozeny–Carman is well known and widely applied to describe the internal bed resistance in terms of overall characteristic parameters of a porous medium. For cylindrical elements with diameter d_f and interstitial bed velocity u , we write:

$$\Delta P = K \mu \frac{16}{d_f^2} \left(\frac{1 - \varepsilon}{\varepsilon} \right)^2 u L \quad (7)$$

Table 2
Calculated $\alpha_D \varepsilon$ for porous stirrer blades

Porosity	0.63	0.74	0.78
$d_f = 8 \mu\text{m}$	1.8	2.3	3.0
Porosity	0.67	0.72	0.77
$d_f = 12 \mu\text{m}$	2.1	3.1	3.0
Porosity	0.72	0.80	
$d_f = 17 \mu\text{m}$	1.9	2.8	
Porosity	0.74	0.84	
$d_f = 22 \mu\text{m}$	2.9	2.3	
Porosity	0.65	0.81	0.86
$d_f = 35 \mu\text{m}$	2.5	1.9	(2.7) vessel limit

Hence, the force balance around the blade inlet area can be written as:

$$\alpha_D \varepsilon \frac{\rho u_T^2}{2} = K \mu \frac{16}{d_f^2} \left(\frac{1 - \varepsilon}{\varepsilon} \right)^2 u L \quad (8)$$

The interstitial velocity u can be calculated from the experiments as L/τ .

K values have been measured for many materials, but none of the correlations in literature represented well our results (e.g. [5–7]). We hence replaced K by an empirical expression that best fitted our own K -data for the fibrous materials:

$$K = K_0 + \alpha \left(\frac{\varepsilon}{1 - \varepsilon} \right)^n \quad (9)$$

whereby the parameters were experimentally and independently determined in stationary laminar flow in another set-up as $K_0 = 2$, $\alpha = 0.053$ en $n = 3$.

The relation between the imposed tip speed u_T and the internal bed velocity u , now finally is:

$$u^{-1} = \frac{\tau'}{\lambda} = \frac{32L}{\alpha_D} \frac{\mu}{\rho d_f^2} \left[2 \frac{(1 - \varepsilon)^2}{\varepsilon^3} + \frac{0.053}{1 - \varepsilon} \right] u_T^{-2} \quad (10)$$

and indeed confirms the earlier experimental finding that $u^{-1} \sim u_T^{-2}$. The value for the product $\alpha_D \varepsilon$ can now be derived from fitting the experimental data to this equation and is around 2.5 (Table 2). No specific pattern can be found in the results. Hence, this value of $\alpha_D \varepsilon = 2.5$ can be used to estimate velocities and contact times in the fiber mat when operated at a particular rotational speed.

5. Mass transfer

Mass transport between fibers and the liquid flow through fiber stacks was experimentally determined with an electrochemical technique [8]. In agreement with boundary layer theory, the Sherwood-number in the examined laminar flow range turned out to be proportional to $Re^{1/2} Sc^{1/3}$. Proportionality factors were determined for fibrous materials with porosity values between 0.65 and 0.80 and fiber diameters between 17 and 35 μm . The porosity influence could be incorporated in the final correlation, expressing the

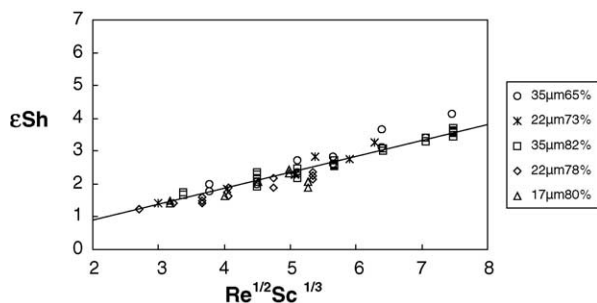


Fig. 7. Rescaled experimental values of the Sherwood number for all samples.

convective mass transfer in a fibrous medium submitted to a low-Re flow regime as shown in Fig. 7:

$$\varepsilon Sh = 0.47 Re^{1/2} Sc^{1/3} \quad (11)$$

6. Conclusions

Due to high permeability, adequate liquid flow can occur through fibrous materials when rotated at the normal tip speeds. Furthermore, the versatility of fibrous materials in porosity and fiber diameter composition allows establishing a broad range of suitable internal hydrodynamic conditions for a variety of catalytic reactions. When applied in a tank reactor as perfusive and coatable blades of a catalytic stirrer system, fibrous elements exhibit internal residence time

values ranging from below 0.5 up to 500 s, for a (reacting) flow traveling through a stack of 1 cm length. The residence time in the blades scales with the applied stirrer tip speed u_T along u_T^{-2} and is inversely proportional to the square of the fiber diameter. Together with the equation found for mass transfer, these equations allow for design of catalytic stirrers incorporating fibrous mats, provided the intrinsic kinetics on the catalyst are available.

Acknowledgements

This work was supported by the IAP V-3 Program of the Belgian Federal Government and the STWW HYP-CAT Programme of the Flemish Government.

References

- [1] A. Cybulski, J.A. Moulijn, *Structured Catalysts and Reactors*, Marcel Dekker, New York, 1998.
- [2] D.R. Cahela, B.J. Tatarchuk, *Catal. Today* 69 (2001) 33–39.
- [3] Y. Matatov-Meytal, M. Sheintuch, *Appl. Catal. A: Gen.* 231 (2002) 1–16.
- [4] R.K.E. Albers, M.J.J. Houterman, T. Vergunst, E. Grolman, J.A. Moulijn, *AIChE J.* 44 (1998) 2459–2464.
- [5] W.L. Ingmanson, B.D. Andrews, R.C. Johnson, *Tappi J.* 42 (1959) 840–849.
- [6] W.L. Ingmanson, B.D. Andrews, *Journal* 46 (1963) 150–155.
- [7] S.T. Han, *Pulp Paper Mag. Can.* May (1969) 65–77.
- [8] J.R. Selman, C.W. Tobias, *Adv. Chem. Eng.* 10 (1978) 211–318.